NJC

PAPER

View Article Online
View Journal

Check for updates

Cite this: DOI: 10.1039/c9nj02555c

Assessing the influence of phosphine substituents on the catalytic properties of self-stabilised digold(I) complexes with supporting ferrocene phosphinonitrile ligands†

Ondřej Bárta, Ivana Císařová, Jiří Schulz and Petr Štěpnička *

Received 17th May 2019,
Accepted 21st June 2019

DOI: 10.1039/c9nj02555c

rsc.li/njc

Gold(I) phosphine complexes are often used in catalysis, but the role of their auxiliary ligands still remains poorly understood. Thus, building on our previous research, we prepared a series of Au(I) complexes $[Au_2(\mu\text{-}R_2PfcCN)_2][SbF_6]_2$ (fc = ferrocene-1,1′-diyl) to assess the effect of phosphine groups PR_2 on the catalytic properties of these highly catalytically active, dimeric compounds. Catalytic testing in Au-mediated cyclisation of *N*-propargyl amides to 2-substituted 5-methyleneoxazolines showed that weaker donating phosphines gave rise to more active, albeit partly destabilised, catalysts. Nevertheless, thanks to their self-stabilisation by reversible nitrile coordination, $[Au_2(\mu\text{-}R_2PfcCN)_2]^+$ cations readily converted into catalytically active species (by dissociation) and, in addition, remained catalytically active even at very low metal loadings. The experimental results were supported by the trends in $^1J_{PSe}$ coupling constants for $R_2P(Se)fcCN$ as a measure of ligand basicity, and by DFT calculations.

Published on 21 June 2019. Downloaded by Chalmers Tekniska Hogskola on 7/5/2019 12:47:32 PM.

Introduction

Research interest in homogeneous gold-catalysed reactions has increased tremendously in recent decades, leading to useful synthetic methods that efficiently exploit the ability of gold(I) species to activate unsaturated bonds *via* coordination.[1] However, the influence of the auxiliary ligands (L) on the performance of the presumed active species LAu^+ has been mostly overlooked.[2]

Recently, we have prepared dimeric complexes $[Au_2(\mu(P,N)\text{-}L)_2]X_2$, where L is 1′-(diphenylphosphino)-1-cyanoferrocene (**1c**)[3] or 2-(diphenylphosphino)benzonitrile and X is a weakly coordinating anion. These compounds are bench-stable and silver-free[4,5] instant precursors of highly active Au(I) catalysts,[6,7] which resemble the commonly used pre-catalysts $[(R_3P)Au(MeCN)]X$,[2d,4] although their phosphinonitrile ligands provide both a strongly coordinating donor moiety and a labile donor group. With previous work,[8] we have shown that the nitrile group plays a key role in determining the catalytic activity of $[Au_2(\mu\text{-}L)_2]X_2$ complexes. In this study, we focus on the influence of phosphine substituents on the catalytic properties of complexes $[Au_2(\mu(P,N)\text{-}R_2PfcCN)_2][SbF_6]_2$ (fc = ferrocene-1,1′-diyl) using Au-mediated cyclisation of *N*-propargylamides to 5-methyleneoxazolines[9] as a test reaction and phosphine selenides to probe the ligand properties.[10]

Results and discussion

To achieve the goals of this study, additional phosphinonitrile ligands $R_2PfcC{\equiv}N$ (**1**) bearing electronically distinct phosphino substituents [R = iso-propyl (**a**), cyclohexyl (Cy, **b**), and 2-furyl (Fur; **d**)] were prepared to complement the archetypal representative **1c**.[3,6] These compounds were obtained by successive lithiation/functionalisation[11] of 1,1′-dibromoferrocene (**2**), as shown in Scheme 1.[12] Ligands **1** were subsequently converted into chloridogold(I) complexes **5** and then into the target digold(I) complexes $[Au_2(\mu(P,N)\text{-}R_2PfcCN)_2][SbF_6]_2$ (**6**). To gain further insight into the donor properties of ligands **1**, selenides **7** were prepared from free phosphines *via* reactions with KSeCN[13] (Scheme 1).

In addition, syntheses performed on a relatively large scale, especially during the first steps, enabled us to isolate and ultimately characterise an intensely purple minor side-product detected[12] during the transformation of **2** into **3** as the cyanamide $(Brfc)_2C{=}NC{\equiv}N$ (**4**). This compound arises by addition of the intermediate BrfcLi to the cyanide group in the already formed **3**, followed by reaction of the resulting imine salt with TsCN (see the ESI†).

All compounds have been characterised by spectroscopic methods and by elemental analysis. In their NMR spectra,

Department of Inorganic Chemistry, Faculty of Science, Charles University, Hlavova 2030, 128 40 Prague, Czech Republic. E-mail: petr.stepnicka@natur.cuni.cz

† Electronic supplementary information (ESI) available: Experimental details including structure determination, additional structural diagrams and kinetic plots, details on DFT calculations, copies of the NMR spectra and coordinates of DFT computed structures. CCDC 1909789–1909795. For ESI and crystallographic data in CIF or other electronic format see DOI: 10.1039/c9nj02555c

Published on 21 June 2019. Downloaded by Chalmers Tekniska Hogskola on 7/5/2019 12:47:32 PM.

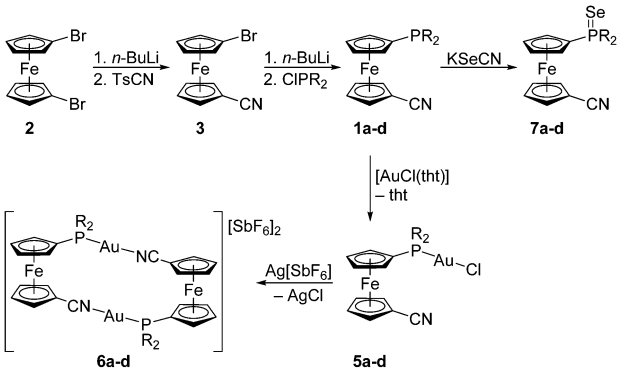

Scheme 1 Synthesis of complexes **6** and phosphine selenides **7** [R = isopropyl (**a**), cyclohexyl (**b**), phenyl (**c**), and 2-furyl (**d**); Ts = 4-toluenesulfonyl, tht = tetrahydrothiophene]. Note: only compounds **1c**, **5c** and **6c** have been previously reported.

phosphines **1** showed characteristic signals due to the ferrocene unit and to the phosphine substituents; the ^{31}P NMR signals were observed at δ_P 0.1 (**1a**), −8.0 (**1b**), −17.7 (**1c**)[3] and −66.1 (**1d**) ppm. The ^{13}C NMR signals of the CN groups occurred at $\delta_C \approx 120$, while the IR bands attributable to the $\nu_{C\equiv N}$ modes were observed in the narrow range of 2224–2228 cm^{-1}. Coordination of **1**, yielding chloridogold(I) complexes **5**, resulted in a shift of the ^{31}P NMR signals to a lower field, while the signature of the CN substituents changed only marginally. Upon converting **5** into dimers **6**, the ^{31}P resonances shifted to slightly higher fields, while the $\nu_{C\equiv N}$ bands moved to higher energies.[14]

The molecular structures of **1d**, **5d** and **6d** are depicted in Fig. 1; those of the chloridogold(I) complexes **5a**, **5b** and **5d** and of dimer **6b** are presented in the ESI,† along with additional data and structural diagrams. The gold(I) ions in complexes **5** are linearly coordinated (Cl–Au–P = 175–177°), showing shorter

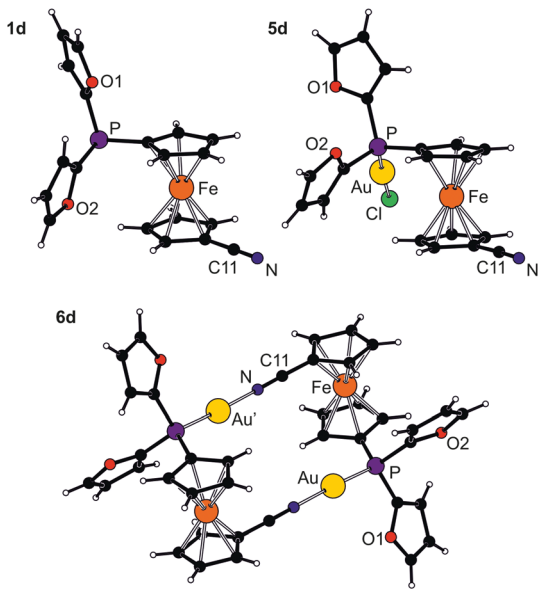

Fig. 1 View of the molecular structures of **1d**, **5d** and of the complex cation in the structure of **6d**. Additional plots and further structural data are available in the ESI.†

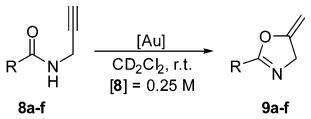

Scheme 2 Au-catalysed cyclisation of propargyl amides **8** to oxazolines **9** [R = Ph (**a**), 4-MeC$_6$H$_4$ (**b**), 4-MeOC$_6$H$_4$ (**c**), 4-ClC$_6$H$_4$ (**d**), 4-CF$_3$C$_6$H$_4$ (**e**), and Cy (**f**)].

Au–P bonds in compounds with weaker donating phosphines due to increased π-back donation (Au–P: 2.2361(6), 2.2319(7), 2.2287(6),[6] and 2.2191(6) Å for **1a–d**, respectively). Although X-ray diffraction analysis confirmed the dimeric nature of **6** in all cases, the structure of **6a** could not be satisfactorily refined due to disorder. The Au–P distances determined for **6b** and **6d** are very close to those determined for **5b** and **5d**, while the CN bond lengths of the coordinated nitrile unit show virtually no difference from those in the respective free phosphines **1**.

Complexes **6** were examined as (pre)catalysts in the Au-catalysed cyclisation of propargyl amides **8** to 5-methylene-4,5-dihydrooxazoles (oxazolines) **9** (Scheme 2).[9] Gratifyingly, the cyclisation of the prototypical substrate **8a** proceeded selectively with all catalysts **6** to give **9a** as the sole product, thus enabling us to monitor the reaction conveniently by ^{1}H NMR spectroscopy (Fig. S7, ESI†). The resulting oxazolines were isolated, but they slowly decomposed when exposed to air.[15]

All pre-catalysts **6** gave full conversions within 3 h when used at 1 mol% Au loading (25 °C, [**8a**]$_0$ = 0.25 M, CD_2Cl_2). Nonetheless, the catalysts showed different kinetic profiles. In particular, cyclisation reactions with catalysts bearing aromatic phosphine substituents proceeded faster than those with catalysts bearing dialkylphosphine moieties (Fig. 2). Although relatively minor, the difference in performance between the catalysts can be easily demonstrated by comparing the corresponding yields of **9a** after 1 h, which were approximately 90% for **6c** and **6d**, and 70% for **6a** and **6b**. When using the common pre-catalyst [Au(PPh$_3$)(MeCN)][SbF$_6$], the cyclisation reaction also reached full conversion within 3 h, though at an intermediate rate between **6c**/**6d** and **6a**/**6b**. The reaction rates (k) determined by fitting the ln([**8**]/[**8**]$_0$) *vs.* time plots (see ESI†) corroborate this semi-quantitative assessment (Table 1).

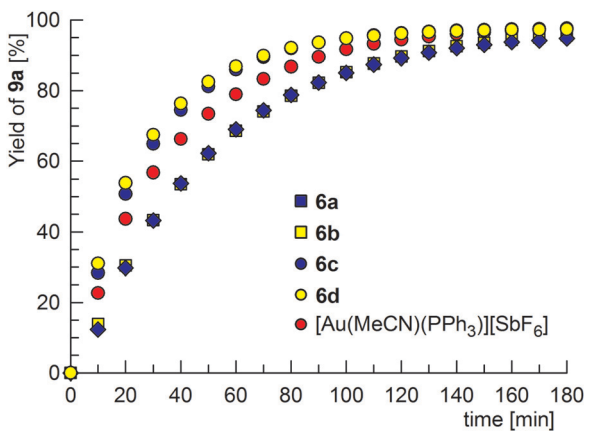

Fig. 2 Kinetic profiles of the cyclisation of **8a** to **9a** catalysed by different Au(I) catalysts ([**8a**]$_0$ = 0.25 M in CD_2Cl_2, 25 °C, [Au] = 1 mol%).

This journal is © The Royal Society of Chemistry and the Centre National de la Recherche Scientifique 2019

Published on 21 June 2019. Downloaded by Chalmers Tekniska Hogskola on 7/5/2019 12:47:32 PM.

Table 1 Reaction rates of the model cyclisation of substrate **8a** and additional parameters illustrating the properties of ligands **1** and their Au(I) complexes

	Ligand				
Parameter	**1a**	**1b**	**1c**	**1d**	PPh_3
k^a [10^{-3} min^{-1}]	20.8(2)	20.2(2)	32.5(7)	32.9(10)	25.7(7)
ν_{CN} for **1**^{b} [cm^{-1}]	2224	2225	2225[e]	2228	n.a.
ν_{CN} for **6**^{b} [cm^{-1}]	2263	2256	2273[f]	2274	n.a.
Au–P for **6**^{c} [Å]	n.a.	2.242 (av.)	2.225(2)[f]	2.2139(7)	2.228(1)[g]
Au–N for **6**^{c} [Å]	n.a.	2.050 (av.)	2.035(4)[f]	2.032(2)	2.038(5)[g]
E_{dis} for **6**^{d} [kcal mol^{-1}]	27.4	26.8	29.4	32.9	n.a.
$^1J_{SeP}$ for **7** ($CDCl_3$) [Hz]	715	708	741	777	735[h]

[a] Rate constants of the cyclisation of **8a**. Conditions: $[\mathbf{8}]_0$ = 0.25 M in CD_2Cl_2, 1 mol% Au, and 25 °C. Determined from fitting the kinetic profile in the range of 10–60 min. [b] IR spectra recorded in Nujol mulls. [c] Au–P and Au–N distances from X-ray diffraction analysis at 120 or 150 K. [d] Dissociation energies of isolated dimeric cations calculated by DFT. [e] Ref. 3. [f] Ref. 6. [g] Data on $[(Ph_3P)Au(MeCN)][SbF_6]$ from ref. 16. [h] Ref. 17.

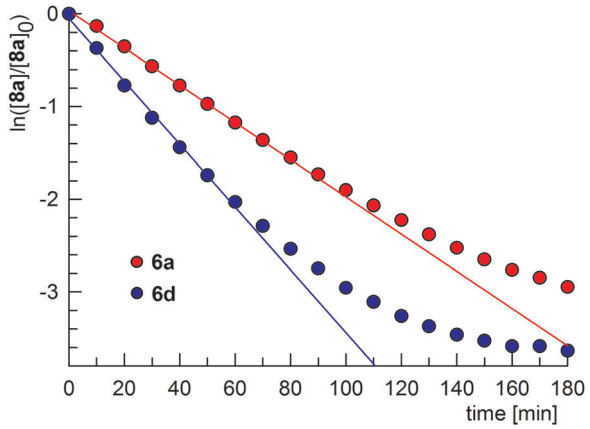

Fig. 3 Kinetic ($\ln([\mathbf{8a}]/[\mathbf{8a}]_0)$ *vs.* time) plots of representative catalysts **6a** and **6d** illustrating the departure from first-order behaviour.

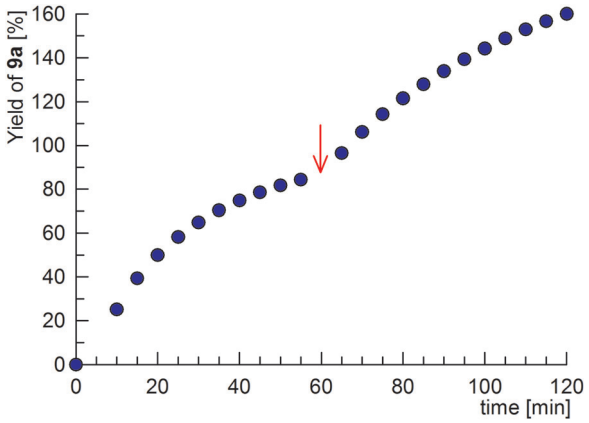

Fig. 4 Kinetic profile of the cyclisation of **8a** to **9a** mediated by **6d** in which additional **8a** was added after 1 h of reaction (indicated by a red arrow).

Further measurements indicated that the cyclisation is a first-order reaction with respect to the amide substrate (Fig. 3 and Fig. S8, ESI†). Our findings thus contrast with previous measurements using $[Au(PR_3)(OTf)]$ catalysts, which showed a linear decrease in substrate concentration over time (0th order reaction).[2b] Such divergence, which was confirmed by independent experiments using the $[Au(PPh_3)(OTf)]$ catalyst, may be attributed to the anion effect ($[SbF_6]^-$ *vs.* OTf^-)[18] and, mainly, to the stabilising role of the nitrile moiety in **6**, whose coordination can prevent decomposition and the formation of gold(I) bis(phosphine) cations or similar species.[19]

The $\ln([\mathbf{8}]/[\mathbf{8}]_0)$ *vs.* time plots for catalysts **6** were linear until approximately 90% conversion, subsequently departing from a linear relationship, which was more pronounced for the faster reacting catalysts (see Fig. 3 and Fig. S8, ESI†). This observation can be explained by catalyst decomposition, which is faster for the more reactive catalysts. Indeed, when an additional equivalent of substrate **8a** was added to the reaction mixture at nearly full conversion (90%), using 1 mol% Au in the form of **6d**, the reaction continued but at a slower rate (approximately half of the original reaction rate, see Fig. 4).

Additional reaction tests performed with the most efficient catalyst **6d** showed that the cyclisation is a first-order reaction in the catalyst (Fig. S9 and S10, ESI†). Using 2 mol% of Au, the reaction with catalyst **6d** reached full conversion within 1 h but proceeded reasonably well also under much lower catalyst loadings (*cf.* 65% conversion after 3 h with 0.25 mol% Au). Remarkably, upon further decreasing the catalyst amount, the reaction slowed down but did not stop. Even with as little as 0.03 mol% Au, the NMR yield of **9a** was 4% after 90 min, and the reaction followed pseudo first-order kinetics. In other words, we have not observed any threshold value below which the reaction did not proceed.[20] Instead, the reaction rate tended towards zero at very low catalyst loadings (Fig. 5). This observation again reflects the unique self-stabilising ability of the $Au(\mathbf{1})^+$ species resulting from reversible dimerisation by nitrile coordination. Unsurprisingly, strongly binding ligands affected this process. For instance, addition of a stoichiometric amount of chloride ions, which coordinate Au(I) stronger than alkynes,[19] stopped the reaction, even at a relatively high catalyst concentration (1 mol% Au, $[\mathbf{8a}]_0$ = 0.25 M).

On the whole, our results confirm that weaker donating auxiliary ligands give rise to more active gold catalysts.[21] The reduced donor ability (basicity) of **1c** and **1d** is clearly expressed by the relatively large $^1J_{PSe}$ coupling constants (see Table 1), which also suggest that the cyano substituent further reduces the donor properties of the entire ferrocene ligand (compare the $^1J_{PSe}$ value of **1d** in Table 1 with the value for $FcP(Se)Ph_2$ of

Published on 21 June 2019. Downloaded by Chalmers Tekniska Hogskola on 7/5/2019 12:47:32 PM.

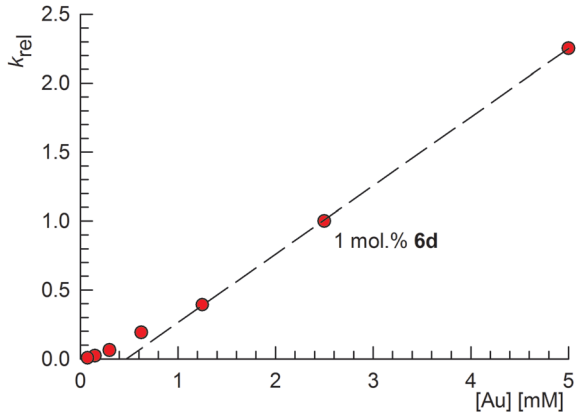

Fig. 5 Variation of the relative reaction rate ($k_{rel} = k/k_{1mol\%}$) as a function of the concentration of gold in the reaction system ([**8a**]$_0$ = 0.25 M, catalyst **6d**).

733 Hz,[22] Fc = ferrocenyl). As stronger π-accepting ligands, **1c** and **1d** form relatively shorter (stronger) Au–P bonds in dimers **6** while the $\nu_{C\equiv N}$ bands of **6c** and **6d** are shifted to higher energies due to stronger σ-donation from a weakly antibonding molecular orbital corresponding to the lone pair at nitrogen.[23] This blue shift in $\nu_{C\equiv N}$ frequencies is in line with the strengthening of the CN → Au interactions suggested by DFT calculations, which show that the energy cost associated with the dissociation of dimers **6** ($[Au_2(\mu\text{-}\mathbf{1})_2]^{2+} \rightarrow 2[Au(\mathbf{1}\text{-}\kappa P)]^+$) is larger in complexes with weaker donating phosphine ligands (**1b** < **1a** < **1c** < **1d**).

Another set of experiments aimed at elucidating the influence of the acyl groups in the substrate on the course of the cyclisation has been performed with amides bearing different substituents in position 4 of their benzene rings, compounds **8a–e**, and with their aliphatic analogue **8f** (Scheme 2). All aromatic amides were efficiently converted into the corresponding oxazolines when using **6d** as the pre-catalyst (1 mol% Au) under standard conditions (Fig. 6). Even though compounds with electron-withdrawing substituents reacted faster, the reaction rates (Table 2) did not correlate with Hammett's constants or with analogous substituent parameters.

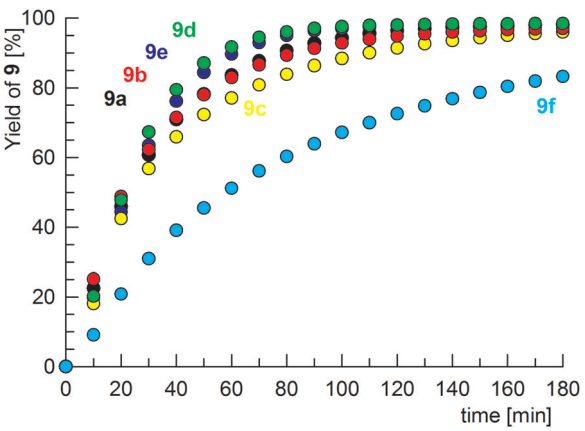

Fig. 6 Kinetic profiles of the cyclisation reactions of different substrates: black – **8a**, red – **8b**, yellow – **8c**, **8d** – green, **8e** – blue, and **8f** – cyan. Conditions: [**8**]$_0$ = 0.125 M in CD_2Cl_2, catalyst **6d** (1 mol% Au), and 25 °C.

Table 2 Reactions rates (k) for the cyclisation of different substrates **8**[a]

Substrate	k [10^{-3} min^{-1}]	Substrate	k [10^{-3} min^{-1}]
8a (Ph)	30.9(7)	**8d** (4-ClC_6H_4)	45.5(3)
8b (4-MeC_6H_4)	29.2(11)	**8e** (4-$CF_3C_6H_4$)	41.3(5)
8c (4-$MeOC_6H_4$)	25.1(15)	**8f** (cyclohexyl)	12.4(3)

[a] Conditions: [**8**]$_0$ = 0.125 M, catalyst **6d** (1 mol% Au), and reaction in CD_2Cl_2 at 25 °C. The rate constants were determined by fitting the kinetic profile over the range 10–60 min.

Indeed, such behaviour matches the proposed reaction mechanism,[9a] which suggests that the coordination of the substrate's triple bond is the initial step. Although the acyl groups in **8** are located far from the alkyne moiety (and are separated by the non-conjugated methylene spacer), they can nevertheless affect other reaction steps (for instance, the nucleophilic attack of the oxygen atom on the coordinated triple bond or the final protodeauration by changing the partial charge at the oxygen atom and the acidity of the NH hydrogen). Conversely, the reaction with amide **8f** was considerably slower (≈80% conversion in 3 h), presumably due to the lack of stabilisation of the reaction intermediates by π-conjugation.

Conclusions

The presence of a nitrile group as a secondary donor moiety in the molecules of supporting phosphine ligands **1** markedly influences the catalytic behaviour of cations $[Au_2(\mu\text{-}\mathbf{1})_2]^{2+}$. These cations, which become active catalysts by simple dissociation, can form again and thus stabilise the active species. Such self-stabilisation markedly differentiates $[Au_2(\mu\text{-}\mathbf{1})_2]^{2+}$ cations from their conventional counterparts $[(R_3P)Au(R'CN)]^+$, primarily by their high catalytic activity, which is preserved even at very low catalyst concentrations, and by the minimised influence of the counter ion (anion coordination is suppressed by the competing nitrile donor). The catalytic activity of $[Au_2(\mu\text{-}\mathbf{1})_2]^{2+}$ can be further increased by introducing less basic phosphine moieties into the structure of the supporting phosphinonitrile ligands. However, such a change decreases the overall chemical stability of the $[Au_2(\mu\text{-}\mathbf{1})_2]^{2+}$ species. Therefore, a judicious choice of the phosphine substituents is essential for achieving optimal catalytic results with these catalysts.

Conflicts of interest

There are no conflicts to declare.

Acknowledgements

This research was supported by the Czech Science Foundation (project no. 17-02495S), by the Grant Agency of Charles University (project no. 130317), and by the Charles University Research Centre program (project no. UNCE/SCI/014).

 This journal is © The Royal Society of Chemistry and the Centre National de la Recherche Scientifique 2019

Published on 21 June 2019. Downloaded by Chalmers Tekniska Hogskola on 7/5/2019 12:47:32 PM.

Notes and references

1 Selected reviews: (*a*) G. Dyker, *Angew. Chem., Int. Ed.*, 2000, **39**, 4237–4239; (*b*) A. S. K. Hashmi, *Chem. Rev.*, 2007, **107**, 3180–3211; (*c*) A. Fürstner and P. W. Davies, *Angew. Chem., Int. Ed.*, 2007, **46**, 3410–3449; (*d*) Z. Li, C. Brouwer and C. He, *Chem. Rev.*, 2008, **108**, 3239–3265; (*e*) N. D. Shapiro and F. D. Toste, *Synlett*, 2010, 675–691; (*f*) R. Dorel and A. M. Echavarren, *Chem. Rev.*, 2015, **115**, 9028–9072; (*g*) D. Pflästerer and A. S. K. Hashmi, *Chem. Soc. Rev.*, 2016, **45**, 1331–1367; (*h*) W. Zi and F. D. Toste, *Chem. Soc. Rev.*, 2016, **45**, 4567–4589; (*i*) A. S. K. Hashmi and F. D. Toste, *Modern Gold Catalyzed Synthesis*, Wiley-VCH, Weinheim, 2012; (*j*) F. D. Toste and V. Michelet, *Gold Catalysis: An Homogeneous Approach*, Imperial College Press, London, 2014.

2 (*a*) D. J. Gorin, B. D. Sherry and F. D. Toste, *Chem. Rev.*, 2008, **108**, 3351–3378; (*b*) W. Wang, G. B. Hammond and B. Xu, *J. Am. Chem. Soc.*, 2012, **134**, 5697–5705; (*c*) D. Malhotra, G. B. Hammond and B. Xu, *Top. Curr. Chem.*, 2015, **357**, 1–23; (*d*) B. Ranieri, I. Escofet and A. M. Echavarren, *Org. Biomol. Chem.*, 2015, **13**, 7103–7118; (*e*) C. A. Gaggioli, G. Ciancaleoni, D. Zuccaccia, G. Bistoni, L. Belpassi, F. Tarantelli and P. Belanzoni, *Organometallics*, 2016, **35**, 2275–2285; (*f*) A. H. Christian, Z. L. Niemeyer, M. S. Sigman and F. D. Toste, *ACS Catal.*, 2017, **7**, 3973–3978.

3 K. Škoch, I. Císařová and P. Štěpnička, *Inorg. Chem.*, 2014, **53**, 568–577.

4 H. Schmidbaur and A. Schier, *Z. Naturforsch.*, 2011, **66b**, 329–350.

5 Additional references: (*a*) D. Wang, R. Cai, S. Sharma, J. Jirak, S. K. Thummanapelli, N. G. Akhmedov, H. Zhang, X. Liu, J. L. Petersen and X. Shi, *J. Am. Chem. Soc.*, 2012, **134**, 9012–9019; (*b*) A. Homs, I. Escofet and A. M. Echavarren, *Org. Lett.*, 2013, **15**, 5782–5785; (*c*) Z. Lu, J. Han, G. B. Hammond and B. Xu, *Org. Lett.*, 2015, **17**, 4534–4537.

6 K. Škoch, I. Císařová and P. Štěpnička, *Chem. – Eur. J.*, 2015, **21**, 15998–16004.

7 B. Michelet, D. Lebœuf, C. Bour, K. Škoch, F. Horký, P. Štěpnička and V. Gandon, *ChemPlusChem*, 2017, **82**, 442–448.

8 K. Škoch, I. Císařová, J. Schulz, U. Siemeling and P. Štěpnička, *Dalton Trans.*, 2017, **46**, 10339–10354.

9 (*a*) A. S. K. Hashmi, J. P. Weyrauch, W. Frey and J. W. Bats, *Org. Lett.*, 2004, **6**, 4391–4394; (*b*) A. S. K. Hashmi, M. Rudolph, S. Schymura, J. Visus and W. Frey, *Eur. J. Org. Chem.*, 2006, 4905–4909; (*c*) A. S. K. Hashmi, A. M. Schuster and F. Rominger, *Angew. Chem., Int. Ed.*, 2009, **48**, 8247–8249; (*d*) J. P. Weyrauch, A. S. K. Hashmi, A. Schuster, T. Hengst, S. Schetter, A. Littmann, M. Rudolph, M. Hamzic, J. Visus, F. Rominger, W. Frey and J. W. Bats, *Chem. – Eur. J.*, 2010, **16**, 956–963.

10 (*a*) C. A. Tolman, *Chem. Rev.*, 1977, **77**, 313–348; (*b*) D. W. Allen and B. F. Taylor, *J. Chem. Soc., Dalton Trans.*, 1982, 51–54; (*c*) A. Muller, S. Otto and A. Roodt, *Dalton Trans.*, 2008, 650–657; (*d*) U. Beckmann, D. Süslüyan and P. C. Kunz, *Phosphorus, Sulfur Silicon Relat. Elem.*, 2011, **186**, 2061–2070.

11 (*a*) I. R. Butler and R. L. Davies, *Synthesis*, 1996, 1350–1354; (*b*) P. Štěpnička in *Ferrocenes: Ligands, Materials and Biomolecules*, ed. P. Štěpnička, Wiley, Chichester, 2008, ch. 5, pp. 177–204.

12 K. Škoch, I. Císařová, F. Uhlík and P. Štěpnička, *Dalton Trans.*, 2018, **47**, 16082–16101.

13 P. Nicpon and D. W. Meek, *Inorg. Chem.*, 1966, **5**, 1297–1298.

14 Coordination of a nitrile moiety is typically associated with a shift of the $\nu_{C\equiv N}$ band towards higher energies as the result of electron density removal from a weakly antibonding molecular orbital (lone pair at N). π-Back donation, which increases the population of antibonding orbitals, is rather weak. For references, see: K. Nakamoto, *Infrared and Raman Spectra of Inorganic and Coordination Compounds, Part B: Applications in Coordination, Organometallic, and Bioinorganic Chemistry*, Wiley, New York, 5th edn, 1997, sect. III-15, pp. 105–115.

15 A. S. K. Hashmi, M. C. B. Jaimes, A. M. Schuster and F. Rominger, *J. Org. Chem.*, 2012, **77**, 6394–6408.

16 E. Herrero-Gómez, C. Nieto-Oberhuber, S. López, J. Benet-Buchholz and A. M. Echavarren, *Angew. Chem., Int. Ed.*, 2006, **45**, 5455–5459.

17 R. P. Pinnell, C. A. Megerle, S. L. Manatt and P. A. Kroon, *J. Am. Chem. Soc.*, 1973, **95**, 977–978.

18 (*a*) D. Zuccaccia, L. Belpassi, A. Macchioni and F. Taranteli, *Eur. J. Inorg. Chem.*, 2013, 4121–4135; (*b*) M. Jia and M. Bandini, *ACS Catal.*, 2015, **5**, 1638–1652; (*c*) J. Schiessl, J. Schulmeister, A. Doppiu, E. Wörner, M. Rudolph, R. Karch and A. S. K. Hashmi, *Adv. Synth. Catal.*, 2018, **360**, 2493–2502.

19 A. Zhdanko, M. Ströbele and M. E. Maier, *Chem. – Eur. J.*, 2012, **18**, 14732–14744.

20 M. Kumar, G. B. Hammond and B. Xu, *Org. Lett.*, 2014, **16**, 3452–3455.

21 Teles *et al.* concluded similarly in their seminal paper from 1998: J. H. Teles, S. Brode and M. Chabanas, *Angew. Chem., Int. Ed.*, 1998, **37**, 1415–1418.

22 B. Milde, M. Lohan, C. Schreiner, T. Rüffer and H. Lang, *Eur. J. Inorg. Chem.*, 2011, 5437–5449.

23 M. L. Kuznetsov, *Russ. Chem. Rev.*, 2002, **71**, 265–282.